Available online at www.sciencedirect.com
ScienceDirect
Journal of Magnetic Resonance 187 (2007) 146–154
JMR Journal of Magnetic Resonance
www.elsevier.com/locate/jmr

Study of diffusion in erythrocyte suspension using internal magnetic field inhomogeneity

Natalia V. Lisitza [a], W.S. Warren [b,1], Yi-Qiao Song [a,*]

[a] Schlumberger-Doll Research, 36 Old Quarry Road, Ridgefield, CT 06877, USA
[b] Department of Chemistry, Princeton University, Princeton, NJ 08544-1009, USA

Received 29 November 2006; revised 13 March 2007
Available online 20 April 2007

Abstract

Transport of water and ions through cell membranes plays an important role in cell metabolism. We demonstrate a novel technique to measure water transport dynamics using erythrocyte suspensions as an example. This technique takes advantage of inhomogenous internal magnetic field created by the magnetic susceptibility contrast between the erythrocytes and plasma. The decay of longitudinal magnetization due to diffusion in this internal field reveals multi-exponential behavior, with one component corresponding to the diffusive exchange of water across erythrocyte membrane. The membrane permeability is obtained from the exchange time constant and is in good agreement with the literature values. As compared to the other methods, this technique does not require strong gradients of magnetic field or contrast agents and, potentially, can be applied *in vivo*.
© 2007 Elsevier Inc. All rights reserved.

Keywords: Diffusive transport; Membrane permeability; Internal magnetic field

1. Introduction

Dynamical processes in tissues, such as diffusion and relaxation, are of great interest and practical significance for characterization of both structures and functions [1]. NMR has been useful to study the movement of water molecules in tissues, in particular, blood [2–12] including the diffusive exchange of intra- and extra-cellular water. Among the parameters used to describe this exchange is a characteristic time τ for molecules to diffuse across the cell membrane, which is related to the membrane permeability. Characterization of water exchange between erythrocytes and plasma by NMR has generally been done on the basis of either relaxation in the presence of contrast agents or diffusion in the presence of applied magnetic field gradients.

The majority of relaxation studies [2–4,8–10,13,14] determine transverse relaxation time (T_2) of water protons using CPMG sequence [15,16] and relaxation-enhancing contrast agents. This method relies on the fact that the intra-cellular proton relaxation times ($T_{1c} = 570$ ms, $T_{2c} = 10$ ms) were found to be shorter than those in the plasma ($T_{1p} = 1700$ ms, $T_{2p} = 100$ ms without contrast agents) in freshly drawn samples [2,10]. A paramagnetic agent can be added to the erythrocyte suspension to shorten T_{1p}. When T_{1p} and T_{1c} are much longer then τ, a water proton exchanges between two compartments several times before it decays, giving rising to a single relaxation time for all protons. In this regime, the exchange time cannot be determined using this method. When the concentration of the contrast agent increases so that $T_{1p} < \tau$, the signal decay exhibits multi-exponential characteristics and τ can be determined using Luz–Meiboom exchange theory [17].

The pulsed gradient spin echo (PGSE) technique [18] has also been used to study exchange in the erythrocyte suspensions [6–8,19]. The apparent diffusion constant

* Corresponding author. Fax: +1 203 438 3819.
E-mail address: ysong@slb.com (Y.-Q. Song).
[1] Present address: Department of Chemistry, Duke University, Durham, NC 27708-0346, USA.

1090-7807/$ - see front matter © 2007 Elsevier Inc. All rights reserved.
doi:10.1016/j.jmr.2007.04.010

(ADC) for water inside erythrocytes is smaller than that in plasma due to a higher intra-cellular protein concentration as well as restriction by cellular membranes. When the diffusion time is shorter than τ, the decay reveals a double-exponential behavior. When the diffusion time becomes comparable to τ, the exchange of water between the erythrocytes and plasma diminishes the difference in ADCs resulting in a single-exponential decay. PGSE-type experiments have been useful in probing tissue microstructure, cell sizes and membrane permeability [5–10,19–25].

Here, we discuss the use of *internal* magnetic field as a novel physical mechanism to study water diffusion in tissues. In a uniform applied magnetic field, a sample consisting of multiple components often exhibits an inhomogeneous field inside the sample due to the different magnetic susceptibilities of the individual components. Signal decay due to diffusion in the internal field (DDIF) has been used to measure pore sizes of rocks [26–28]. In biological tissues, the internal field may arise as a result of susceptibility variations among cells or cellular compartments [29–35]. In blood, the susceptibility difference between erythrocytes and plasma is a major source of the internal field that causes the proton Larmor frequency inside and outside the erythrocytes to be significantly different. In addition, there is a chemical shift difference between water protons inside and outside the erythrocytes [12]. The DDIF technique utilizes these factors to create an imbalance of spin magnetization between inside and outside of erythrocytes and then monitors water exchange across the membrane.

In this study, we apply the DDIF method to explore water diffusion in erythrocyte suspensions. We show that the DDIF signal decay reveals a multi-exponential behavior and the different decay components directly probe the diffusion dynamics, i.e. diffusion within the erythrocytes and exchange between the erythrocytes and plasma. The exchange time constant obtained by DDIF is in good agreement with the literature values [4,6,9,36]. This method might be useful to study more complicated tissues such as muscle and brain.

2. Theory and background

When an inhomogeneous material is subject to a uniform external field B_0, the magnetic field inside the pore space is not uniform, $B(r) = B_0 + B^{\mathrm{i}}(r)$, and the internal field $B^{\mathrm{i}}(r)$ is spatially dependent [37]. The key characteristics of the internal field are that its range is finite, and the length scale of its variation is a signature of the underlying structure [38,39]. This is in contrast to the PGSE method where the length scale is dictated by the applied gradient. DDIF often uses the stimulated echo sequence [40]:

$$\frac{\pi}{2}\text{–}t_{\mathrm{e}}\text{–}\frac{\pi}{2}\text{–}t_{\mathrm{d}}\text{–}\frac{\pi}{2}\text{-detection} \tag{1}$$

where t_{e} is the encoding time and t_{d} the diffusion time. The internal field is present throughout the experiment and no external field gradient is applied. The first two $\pi/2$ pulses encode the internal field by the precession phase ($\Phi = \gamma B^{\mathrm{i}} t_{\mathrm{e}}$) and store it as either $\sin(\Phi)$ or $\cos(\Phi)$ [28]. For the experiments reported here, we selected the sine modulation using phase cycling [27]. After the second pulse, the diffusion of water molecules across regions with different B^{i} reduces the amplitude of the spatial magnetization profile. A stimulated echo is detected after the third pulse and the signal decay is measured as a function of t_{d}. This technique has been applied to many porous materials [39,41].

The essence of DDIF is to induce a spatial pattern of the magnetization to mimic the spatial pattern of the internal field. The measured decay time constant will reflect the diffusion dynamics of the underlying system. For example, suppose two regimes are separated by a membrane and the magnetic field in the two regimes are different. DDIF will produce an initial magnetization difference between the two regimes. Then, during the t_{d} period, the diffusion through the membrane between the two regimes will reduce the magnetization difference and contribute to the signal decay. The time constant of such decay can be a direct measure of the diffusion dynamics and membrane permeability.

Erythrocytes are the major component of blood and they are disk-shaped cells with a diameter of about 8 μm, a width of 2 μm and a thickness of 0.5 μm. The membranes of erythrocytes are permeable for water. In a static erythrocyte suspension, the presence of cell packing structure in combination with the high concentration of hemoglobin in cells gives rise to a susceptibility difference that dominates the magnetic field distribution. The internal field in such a sample exhibits three major characteristics: a spatially non-uniform field inside the erythrocytes, non-uniform field in the plasma, and the field difference between inside and outside the erythrocytes. From comparison with the case of inorganic porous media, we expect that the DDIF experiment is able to determine both the size of the erythrocytes and the length scale of the plasma region (the distance between the erythrocytes). Furthermore, due to the field difference between inside and outside erythrocytes, the DDIF experiment creates a magnetization imbalance across the membrane. This magnetization imbalance is equilibrated by water exchange, the exchange time constant being directly related to the membrane permeability.

In a rotating sample of erythrocyte suspension, the susceptibility broadening can be removed [11,35] and a water chemical shift difference (0.05 ppm) is found between erythrocytes and plasma [12]. In fact, this type of chemical shift difference has been used to directly measure the membrane permeability [42]. The DDIF experiment does not distinguish between the different contributions to proton frequency and utilizes the total phase acquired in the encoding period. In the following discussion, we will use the term "internal field" to include all sources of frequency modulation mentioned above. In addition, it has been found that the erythrocytes tend to align in a uniform magnetic field with the long axis parallel to the field [7,43–45].

As a consequence of this alignment, the "diffusion–diffraction" phenomenon [46] is observed in blood [7,47,48]. Such alignment might affect the detailed field distribution in the erythrocyte suspension. However, the qualitative characteristics of the internal field important for DDIF are likely to remain.

The diffusion dynamics in a coupled multi-compartments system has been described in several theoretical papers (e.g. [9,35,49]). Ref. [49] explicitly evaluates diffusion eigenmodes and is used to interpret the DDIF result because only a few eigenmodes are important in a DDIF experiment. This formalism is compatible with others [9,35] based on diffusion propagator. The spatial character of the eigenfunctions is also very helpful in connecting DDIF results with specific diffusion dynamics and cell structure to gain insight into the underlying physical processes.

3. Materials and methods

3.1. Samples

Fresh feline blood heparinized to avoid clotting is used to make three samples: a packed erythrocyte sample, a crushed cell sample, and a plasma sample. To avoid settling of the erythrocytes during NMR measurements, the packed erythrocyte sample is obtained by centrifugation of the fresh blood sample (Beckman Coulter Avanti J-25) at 6000 rpm (10,000*g*) for 30 min, and then the plasma and buffy coat are removed. The resulting suspension of erythrocytes is washed twice with an isotonic phosphate-buffered saline solution (pH 7.4), and centrifuged as above to remove the surfactant. The preparation procedure is adopted from Higashi et al. [44]. The final hematocrit is approximately 60%.

The crushed cell sample is prepared by stirring erythrocyte suspension in a small vial filled with purified glass beads of 1 mm diameter for 10 min. The vigorous agitation of the beads broke up cell membranes in a similar fashion as a homogenizer. The mixture is then centrifuged at 6000 rpm (10,000*g*) and the supernate is collected as the sample. The resulting sample has a similar protein concentration (uniformly distributed) as the erythrocyte sample but does not have the cell packing structure. Plasma sample is filtered before use. All samples are put into 5 mm NMR tubes and kept in a water bath at 25 °C for 30 min for temperature stabilization prior to NMR experiments.

3.2. NMR experiments

NMR experiments are performed at 25 °C on a Bruker DMX console at a proton Larmor frequency of 400.1 MHz. A few drops of D_2O are added to the samples to allow the use of deuterium lock. In DDIF experiments the intensity of the stimulated echo is measured as a function of t_d, the latter is varied from 100 μs to 8 s, logarithmically. The encoding time t_e is tested for the range of 0.3–25 ms. Experiments with $t_e = 1$, 2 and 3 ms are also performed with a frequency-selective first pulse. Spin–lattice relaxation is measured separately with an inversion recovery sequence. For all experiments, the recycle delay is 20 s.

In blood samples, there are usually two species of protons from water and macromolecules (e.g. hemoglobin). The two species experience different amount of encoding and contribute to different parts of the echo in time domain. The signals from these two species can be separated by using a frequency-selective first pulse in the stimulated echo sequence. We perform water- and protein-selective DDIF experiments by adjusting the transmitter frequency to that of the water or protein (1.5 kHz (3.8 ppm) from water), respectively. We also perform non-selective DDIF experiments with all three short pulses. The durations of the selective and non-selective $\pi/2$ pulses are 800 and 10 μs, respectively.

Since the DDIF signal decays as a sum of the exponential functions, Laplace inversion algorithm [50] is used to analyze the data and extract the distribution of the decay time constants. We call this distribution "DDIF spectrum" throughout the paper. This spectrum represents the amplitudes of the diffusion eigenmodes.

4. Results and discussions

4.1. The presence of internal field in the erythrocyte suspension sample

Figs. 1a and b show the proton frequency spectra of the several samples. The main resonance at zero offset frequency refers to water (Fig. 1a), while the lower-amplitude features around ±2 kHz are from macromolecules, such as proteins [9,10]. The water linewidth in the packed erythrocyte sample is 70 Hz (Fig. 1b), contributed by the following factors: (1) chemical shift difference (20 Hz at 400 MHz) between water in erythrocytes and plasma [12]; (2) frequency shift due to susceptibility difference between erythrocytes and plasma [11,51,52]; (3) spectral broadening due to field variation within individual erythrocyte and plasma compartments. Fig. 1b shows the water resonance in the crushed cell sample with a linewidth of 15 Hz, similar to that of the plasma (10 Hz), and much narrower than that of the erythrocyte suspension sample (70 Hz). This confirms that the linewidth of the static erythrocyte suspension is dominated by the susceptibility contrast in the structure of the cell pack.

4.2. Echo shapes in DDIF experiments

Fig. 2a shows the signals as a function of the detection time t_2 for the packed erythrocytes sample for several encoding times. In addition to the stimulated echo positioned at t_e, the signal exhibits a characteristic post-echo with a maximum at 4 ms. This post-echo develops when the encoding time becomes of the order of milliseconds and grows along t_e. This behavior is expected, because

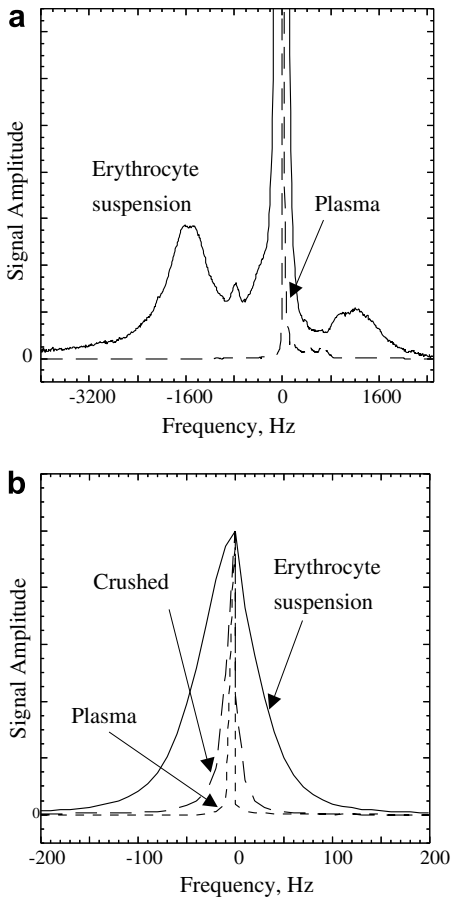

Fig. 1. (a) Frequency spectrum of the erythrocyte suspension sample (solid line) and plasma (dashed line). The main resonance at zero frequency offset is attributed to water, while the lower amplitude features positioned at around −1.6 and 1.2 kHz are from protons of macromolecules, e.g. proteins. (b) The central regions of the frequency spectra of erythrocyte suspension (solid line), crushed cell sample (long dashed line), and the plasma sample (short dashed line). The linewidth was found to be 70, 15, and 10 Hz for erythrocyte suspension, crushed erythrocytes and plasma samples, respectively.

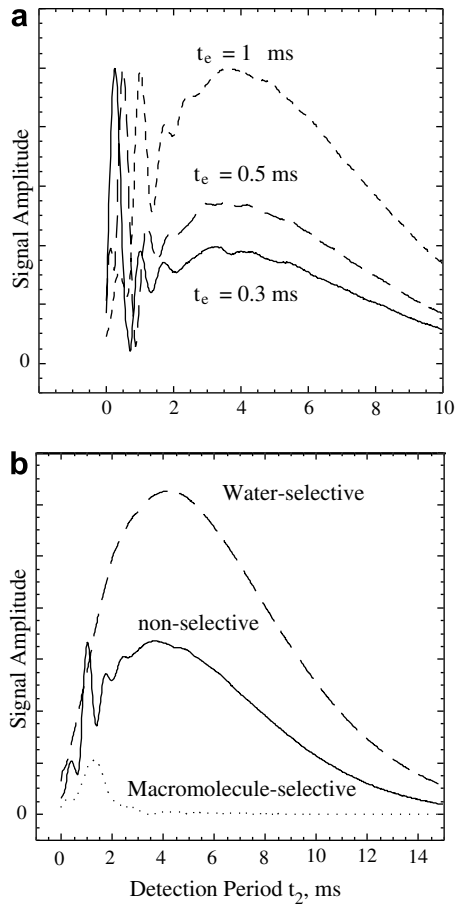

Fig. 2. (a) DDIF signals obtained in the erythrocyte suspension as a function of the detection period, t_2, for three encoding times, t_e, as labeled. (b) Signals obtained for the erythrocyte suspension in a non-selective DDIF experiment (solid line), a water-selective (long dashed line) and a protein-selective (dotted line) experiments as a function of the detection time, t_2. The encoding time, t_e, was 1 ms.

the phase accumulation for the water signal due to internal field during t_e is much less than 2π. Therefore, the maximum of water signal occurs at a fixed time after the third pulse, $\sim\pi/\gamma\Delta B^i$, where ΔB^i is the range of the internal field [27,28] (from Fig. 1a, $\gamma\Delta B^i \sim 70$ Hz). On the other hand, the protons from the proteins acquire larger phase during t_e, so that the maximum of the proteins signal occurs at a time t_e after the third pulse.

Fig. 2b shows the echoes obtained for the erythrocyte suspension sample in water- and protein-selective experiments as compared to the non-selective excitation. In the water-selective experiment, the DDIF signal consists of the post-echo only, while in the protein-selective experiment, only the stimulated echo appears. This behavior confirms that the echo at t_e is due to proteins and the post-echo is mostly due to water. Thus, we can separate the contributions of water and macromolecules to the DDIF signal and observe the diffusion dynamics of water without disturbing the macromolecules.

4.3. DDIF spectrum

Fig. 3a shows the DDIF spectrum of the post-echo data for the erythrocyte suspension sample acquired at $t_e = 1$ ms, together with the T_1 relaxation spectrum obtained by the inversion recovery experiment (IR) and Laplace inversion. The DDIF spectrum consists of several peaks, with the slowest decaying component corresponding to spin–lattice relaxation, as can be seen from a comparison with the T_1 spectrum. In addition to the relaxation peak, there are two faster components in DDIF spectrum.

The difference between IR and DDIF can be understood as follows. The IR experiment was performed by first inverting the spin magnetization and then monitor its recovery. An important aspect to note is that the inverted magnetization profile is spatially uniform. Using Eq. (5) in the Appendix, it can be shown that only the lowest mode (relaxation mode) is detected in such an experiment [53]. Spatial non-uniformity of the RF pulses exists only over the sample size so that the spin magnetization can be regarded as uniform over the cell scale.

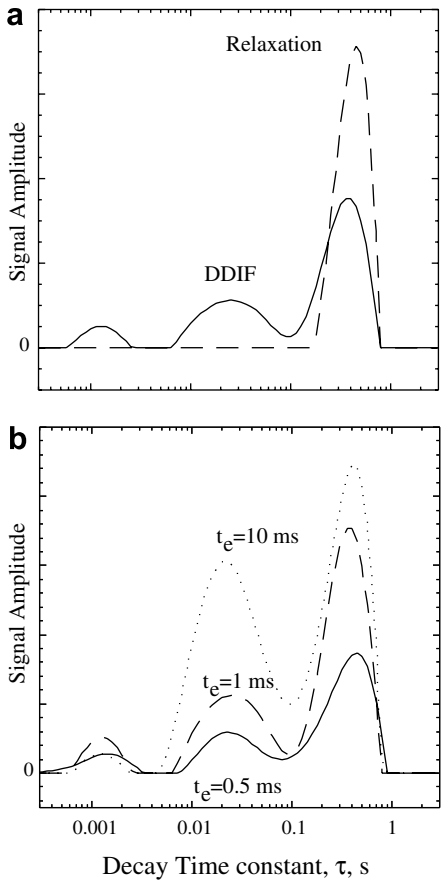

Fig. 3. (a) The DDIF spectrum (solid line) and relaxation spectrum (dashed line) obtained by Laplace inversion for the erythrocyte suspension sample. The encoding time, t_e, was 1 ms for the DDIF experiment. (b) The DDIF spectra obtained in the erythrocyte suspension sample for three encoding times, $t_e = 0.5$ ms (solid line), $t_e = 1$ ms (dashed line), $t_e = 10$ ms (dotted line).

DDIF experiment is very different from IR, since the magnetization is specifically modulated over the characteristic length scale of erythrocytes. As a result, the amplitude of the diffusion eigenmodes (a_n) will be non-zero for many modes. The slowest mode in the DDIF spectra (Fig. 3a) coincides with the T_1 measured in the IR experiment, indicating that it is originated from relaxation. The other two peaks at shorter times in the DDIF spectra are missing in the T_1 spectrum, indicating these modes are directly related to the diffusion process.

Fig. 3b shows DDIF spectra obtained in the erythrocyte sample for several t_e values. The decay time of the fastest component (approx. 1 ms) corresponds to a compartment size of about 3 μm, very close to the width of erythrocytes (2 μm). For a disk-shape compartment such as erythrocytes, there are more eigenmodes corresponding to diffusion across the width (d) than those across the diameter [27,28]. As a result, we expect the DDIF spectrum to be dominated by a peak with the time constant equal to $d^2/\pi^2 D$, where D is the bulk diffusion constant (see Appendix A1 for expressions of eigenmode time constants).

In addition, since the volume ratio of erythrocytes and plasma is 60:40 in the packed erythrocyte sample, the average distance between the erythrocytes in our sample is about 40/60 of the erythrocyte width, $2 * 4/6 \sim 1.3$ μm, assuming the erythrocyte disks are aligned in the magnetic field. Since the magnetic field in the plasma region is non-uniform, one would expect a contribution to the DDIF spectrum from the plasma region with a time constant about 0.2 ms. It is likely that the erythrocytes do not form a packing with perfect long range order, so that the distance between the erythrocytes will vary from its average. For the plasma compartments much smaller than 2 μm, the decay during the encoding period ($t_e = 1$ ms) will suppress the DDIF signal. However, the plasma compartments with erythrocyte–erythrocyte distances close to 2 μm are still partially contribute to the peak in DDIF spectrum at 1 ms. The DDIF experiment alone cannot separate the contributions from erythrocytes and plasma regions since the sizes of these compartments are very similar. We assign DDIF peak at 1 ms to the diffusion mode that corresponds to the diffusion inside the erythrocytes and the plasma.

The spectral peak around 20 ms (Fig. 3b) is found to grow with t_e as the amount of spatial encoding increases. The average decay rate of this peak is estimated to be $1/15\ \mathrm{ms}^{-1}$. The reduction of its amplitude growth rate at $t_e = 10$ ms is likely due to relaxation during the encoding period [27]. A decay time constant of 15 ms corresponds to a diffusion distance of 12 μm (assuming the intra-cellular bulk diffusion constant $D \sim 10^{-5}\ \mathrm{cm}^2/\mathrm{s}$ [27]), which does not match any main structural dimensions of the erythrocyte suspension, such as diameter, width and thickness of erythrocytes and spacing between them. The average value of 15 ms for the decay time agrees relatively well with the exchange time between erythrocytes and plasma (~10 ms) reported in the literature [9,10,36]. We interpret this component as the exchange mode, which corresponds to the water diffusion across the membrane. Taking the volume-to-surface of erythrocytes to be 0.78 μm [54] we obtain a value of $2.1 \pm 0.5 \times 10^{-3}\ \mathrm{cm\ s}^{-1}$ for the membrane permeability. This calculation uses the hematocrit content of 60% in the packed erythrocyte sample, thus, assuming a ratio of 2/3 for the compartment sizes. The value of $2.1 \times 10^{-3}\ \mathrm{cm\ s}^{-1}$ is similar to the previous results for human erythrocytes, such as by Stanisz et al. [9] $-2.8 \times 10^{-3}\ \mathrm{cm\ s}^{-1}$ and Finkelstein [1] $-3 \times 10^{-3}\ \mathrm{cm\ s}^{-1}$. It also falls well into the range of membrane permeability measured for different mammals [21,22,25,55–60].

Although similar to literature values, the membrane permeability obtained from DDIF experiment has a significant range because of the observed distribution of the exchange times. The broadening of the exchange mode may reflect the structural heterogeneity of the cell membrane and consequently, the variations in membrane permeability, or alternatively, it can be due to the heterogeneity of the cell pack. DDIF alone cannot separate the contributions from packing non-uniformity and membrane heterogeneity. This ambiguity is not specific to DDIF technique and a similar

problem exists for the relaxation and diffusion techniques. However, the average membrane permeability can still be obtained from the average exchange time measured by DDIF.

The advantage of the DDIF vs. other techniques for measuring cell membrane permeability and exchange is that DDIF is a direct, non-invasive method and does not require either contrast agents or application of field gradients. DDIF exploits the internal magnetic field, which intrinsically exists in tissues due to structural inhomogeneities and may be used for the measurements both *in vitro* and *in vivo*. The details of the DDIF spectrum can also provide the additional information about local structure of cell membranes. In this regard, the experiments on erythrocytes with altered permeability would be particularly interesting. Also, a quantitative evaluation of the internal field in erythrocyte suspension and detailed numerical simulation of the diffusion dynamics will be useful for a full understanding of DDIF in tissues.

5. Conclusion

A method with a new physical mechanism is presented to probe the structure and dynamics of biological tissues based on the diffusion in the internal magnetic field. We show that the DDIF signal in blood reveals multiple components and directly measures cell sizes and membrane permeability. A theoretical formalism is provided to describe the multi-exponential decay in terms of the eigenmodes of diffusion. Furthermore, the chemical shift difference between species is the additional source of phase encoding in DDIF experiment; in cell systems with significant variations of chemical shifts DDIF measurement of membrane permeability is plausible even without susceptibility contrast.

Acknowledgments

Work at Princeton was supported by the National Institutes of Health under Grant EB-2122, and by the New Jersey Commission on Science and Technology. Work at Schlumberger-Doll Research was partly supported by NIH EB003869-01.

Appendix A

A.1. Theory of diffusion in a coupled pore system

We model the suspension of erythrocytes by considering water occupying two compartments in a one-dimensional (1D) space for its simplicity. The erythrocyte occupies region 1 between $x = 0$ and $x = L$, and plasma occupies region 2 between $x = L$ and $L + K$. The two regions are separated by a permeable membrane at $x = L$.

The dynamics of the longitudinal magnetization within each compartment is governed by the diffusion equation [61]

$$\frac{\partial}{\partial t} m(x,t) = D\nabla^2 m(x,t) \tag{2}$$

where $m(x,t)$ is the magnetization and D is the diffusion coefficient. Here, we have neglected bulk and surface relaxation since it is much slower than the diffusion dynamics in erythrocyte suspensions. The diffusion equation can be solved as an expansion

$$m(x,t) = \sum_{n=0}^{n=\infty} a_n \phi_n(x) \mathrm{e}^{-t/\tau_n} \tag{3}$$

where the eigenmodes $\phi_n(x)$ satisfy the eigenequation

$$-D\nabla^2 \phi_n(x) = \frac{1}{\tau_n} \phi_n(x) \tag{4}$$

The expansion coefficients can be determined by the initial magnetization profile, $m(x,0)$

$$a_n = \int_0^{L+K} \phi_n(x) m(x,0) \mathrm{d}x \tag{5}$$

The eigenmodes of the coupled system are subject to the following boundary conditions

$$\begin{aligned} &\frac{\partial \phi}{\partial x} = 0 \quad \text{at } x = 0, L+K \\ &\frac{\partial \phi^{\mathrm{in}}}{\partial x} = \frac{\partial \phi^{\mathrm{ex}}}{\partial x} = \kappa(\phi^{\mathrm{in}} - \phi^{\mathrm{ex}}) \quad \text{at } x = L \end{aligned} \tag{6}$$

$\kappa = P/D$ is the exchange parameter, P is the membrane permeability using the definition of Herbst and Goldstein, [36]. The indexes "in" and "ex" refer to the intra- and extra-cellular space, respectively. The detailed solution for this problem is described in Ref. [49] and we will discuss a simple case to illustrate the key feature of the relevant eigenmodes. For $K = L$ when the two compartments are equal, the eigenvalues can be obtained through the two equations:

$$\tan(\omega L) = 0 \tag{6a}$$

$$\tan(\omega L) = 2\kappa/\omega \tag{6b}$$

Every eigenfunction splits into symmetric and anti-symmetric ones. For a small κL, the approximate solutions can be obtained:

$$\frac{1}{\tau_n^{\mathrm{s}}} \approx \frac{n^2\pi^2 D}{L^2}, \quad n = 0, 1, 2, \ldots \tag{7a}$$

$$\frac{1}{\tau_0^{\mathrm{a}}} \approx \frac{2P}{L} \tag{7b}$$

$$\frac{1}{\tau_n^{\mathrm{a}}} \approx \frac{n^2\pi^2 D}{L^2} + \frac{4P}{L^2} + \frac{4P^2}{n^2\pi^2 L^2 D}, \quad n \geqslant 1 \tag{7c}$$

For larger κ, Eq. (6) can be solved numerically, shown in Fig. 4. It is worth noting that the symmetric eigenmodes are analogous to the solutions of an isolated pore [53].

The lowest symmetric eigenmode, ϕ_0^{s}, is unique in that it is spatially uniform, and $\omega_0^{\mathrm{s}} = 0$. In realistic systems with finite relaxation, the decay rate of this mode would be determined by the bulk and surface-induced relaxation and the spatial uniformity of the eigenfunction remains

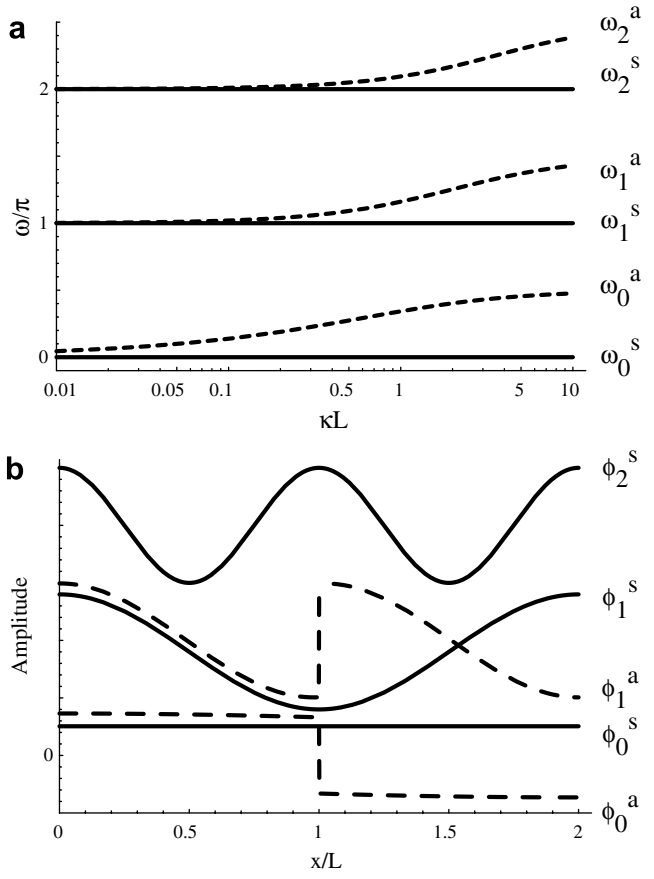

Fig. 4. (a) The eigenvalue ω_n/π as a function of κL for several eignemodes. The superscripts "s" and "a" refer to the symmetric (solid lines) and anti-symmetric (dashed lines) eigenmodes. (b) The spatial profile of the diffusion eigenmodes $\phi_n(x)$, $n = 0,1,2$, as a function of x with $\kappa L = 0.1$, which is similar to the case of the erythrocytes. The membrane is at $x = L$.

[49,62]. For this reason, the lowest mode is often called relaxation mode.

The lowest anti-symmetric eigenmode, ϕ_0^a, is also very different from the other modes, e.g. ϕ_0^s. The most striking feature is the sudden change of its amplitude at the membrane (Fig. 4b). From Eq. (7b), the decay rate of this mode depends on the membrane permeability alone. Thus, we call this eigenmode the "exchange mode", since its dynamics is determined by the exchange between the two compartments, e.g. τ_0^a changes continuously as a function of κ. In the case of a 3D suspension, the compartment size L is to be replaced by the volume-to-surface ratio and Eq. (7b) coincides with the expression for the mean residence time of water inside the erythrocyte given by Herbst and Goldstein [36].

Other higher modes ($n \geqslant 1$) are different from the lowest two modes. The decay rates of these modes are contributed by both diffusion and membrane permeability. Eq. (7c) and Fig. 4a show that diffusion within each compartment is the dominant part of $1/\tau_n$ and the relative change of ω_n as a function of κ is much less than that of ϕ_0^a. It is instructive, therefore, to define these modes ($n \geqslant 1$) as diffusion modes.

A.2. Excitation of diffusion eigenmodes

The general strategy of DDIF is to create a spin magnetization that is not uniform over the length scale of erythrocytes using the internal field. The non-uniform magnetization $m(x,0)$ effectively selects a few eigenmodes including the exchange and diffusion modes. The decay of the magnetization is then measured in order to obtain a spectrum of the modes as a function of the decay time constant. The amplitude of these eigenmodes is determined by the overlap of the respective eigenfunctions and $m(x,0)$, Eq. (5).

In a static erythrocyte suspension sample, the main susceptibility contrast is between the erythrocytes and plasma, thus the field inside erythrocytes is different from that in plasma. Such a field profile can have a significant overlap with the exchange mode, thus, resulting in a finite amplitude of this mode (Eq. (5)). The decay time constant of exchange mode is then a direct measure of the membrane permeability. In addition, since the field inside the erythrocytes or within the plasma region is also non-uniform, there is a non-zero overlap with the eigenfunctions of the diffusion modes.

References

[1] A. Finkelstein, Water Movement Through Lipid Bilayers, Pores, and Plasma Membranes, John Wiley & Sons, New York, 1984.
[2] M.E. Fabry, M. Eisenstadt, Water exchange across red cell membranes II: measurement by nuclear magnetic resonance T_1, T_2, and T_{12} hybrid relaxation: The effects of osmolarity, cell volume, and medium, J. Membr. Biol. 42 (1978) 375–398.
[3] R.M. Kroeker, R.M. Henkelman, Analysis of NMR biological relaxation data with continuous distribution of relaxation times, J. Magn. Reson. 69 (1986) 24–36.
[4] G. Benga, T. Borza, O. Popescu, V.I. Pop, A. Muresan, Water exchange through erythrocyte membranes. Nuclear magnetic resonance studies on resealed ghosts compared to human erythrocytes, J. Membr. Biol. 89 (1986) 127–130.
[5] G. Benga, B.E. Chapman, C.H. Gallagher, N.S. Agar, P.W. Kuchel, NMR-studies of diffusional water permeability of red blood cells from 8 species of marsupials, Comp. Biochem. Physiol. A: Physiology 106 (1993) 515–518.
[6] L.L. Latour, K. Svoboda, P.P. Mitra, C.H. Sotak, Time-dependent diffusion of water in a biological model system, Proc. Natl. Acad. Sci. USA 91 (1994) 1229–1233.
[7] P.W. Kuchel, A. Coy, P. Stilbs, NMR "diffusion–diffraction" of water revealing alignment of erythrocytes in a magnetic field and their dimensions and membrane transport characteristics, Magn. Reson. Med. 37 (1997) 637–643.
[8] G.J. Stanisz, A. Szafer, G.A. Wright, R.M. Henkelman, An analytical model of restricted diffusion in bovine optic nerve, Magn. Reson. Med. 37 (1997) 103–111.
[9] J.G. Stanisz, J.G. Li, G.A. Wright, R.M. Henkelman, Water dynamics in human blood via combined measurements of T_2 relaxation and diffusion in the presence of gadolinium, Magn. Reson. Med. 39 (1998) 223–233.
[10] J.G. Li, J.G. Stanisz, R.M. Henkelman, Integrated analysis of water diffusion and relaxation in blood, Magn. Reson. Med. 40 (1998) 79–88.
[11] J.-H. Chen, B.M. Enloe, Y. Xiao, D.G. Cory, S. Singer, Isotropic susceptibility shift under MAS: origin of the split water resonances in ^{1}H MAS NMR spectra of cell suspensions, Magn. Reson. Med. 50 (2003) 515–521.

[12] D.J. Philp, W.A. Bubb, P.W. Kuchel, Chemical shift and magnetic susceptibility contributions to the intracellular and supernatant resonances in variable angle spinning NMR spectra of erythrocyte suspensions, Magn. Reson. Med. 51 (2004) 441–444.
[13] G.E. Santyr, I. Kay, R.M. Henkelman, M.J. Bronskill, Diffusive exchange analysis of 2-component T_2-relaxation of red-blood-cell suspensions containing gadolinium, J. Magn. Reson. 9 (1990) 500–513.
[14] W.M. Spees, D.A. Yablonskiy, M.C. Oswood, J.J.H. Ackerman, Water proton MR properties of human blood at 1.5 T: magnetic susceptibility, T_1, T_2, T_2^* and non-Lorentzian signal behavior, Magn. Reson. Med. 45 (2001) 533–542.
[15] H.Y. Carr, E.M. Purcell, Phys. Rev. 94 (1954) 630–635.
[16] S. Meiboom, D. Gill, Modified spin-echo method for measuring nuclear relaxation times, Rev. Sci. Instr. 29 (1958) 688–691.
[17] Z. Luz, S. Meiboom, Nuclear magnetic resonance study of the protolysis of trimethylammonium in aqueous solution—order of the reaction with respect to the solvent, J. Chem. Phys. 39 (1963) 366–375.
[18] E.O. Stejscal, J.E. Tanner, Spin diffusion measurement: spin echoes in the presence of a time-dependent field gradient, J. Chem. Phys. 42 (1965) 288–292.
[19] J. Xie, A. Szafer, A.W. Anderson, K.M. Johnson, J.C. Gore, Diffusion measurements of the permeability of the red blood cell membrane, in: Proceedings, ISMRM, 4th Annual Meeting, New York, 1996, p. 1332.
[20] J.E. Tanner, Intracellular diffusion of water, Arch. Biochem. Biophys. Acta 224 (1983) 416–428.
[21] G. Benga, B.E. Chapman, C.H. Gallagher, D. Cooper, P.W. Kuchel, NMR-studies of diffusional water permeability of red blood cells from mavropodud marsupials (kangaroos and wallabies), Comp. Biochem. Physiol. A: Physiology 104 (1993) 799–803.
[22] G. Benga, G.B. Ralston, T. Bordza, B.E. Chapman, C.H. Gallagher, P.W. Kuchel, NMR-studies of diffusional water permeability of red-blood-cells from the echidna tachyglossus-aculeatus, Compar. Biochem. Physiol. B: Biochem. Mol. Biol. 107 (1994) 45–50.
[23] G. Benga, B.E. Chapman, L. Hinds, P.W. Kuchel, Comparative NMR-studies of diffusional water permeability of erythrocytes from some animals introduced to Australia—rat, rabbit and sheep, Comp. Haematol. Inter. 4 (1994) 232–235.
[24] G. Benga, T. Borza, Diffusional water permeability of mammalian red blood cells, Compar. Biochem. Physiol. B: Biochem. Mol. Biol. 112 (1995) 653–659.
[25] G. Benga, P.W. Kuchel, B.E. Chapman, G.C. Cox, I. Ghiran, C.H. Gallagher, Comparative cell shape and diffusional water permeability of red blood cells from Indian elephant (*Elephas maximus*) and man (*Homo sapiens*), Comp. Haematol. Inter. 10 (2000) 1–8.
[26] Y-Q. Song, S. Ryu, P.N. Sen, Determining multiple length scales in rocks, Nature 406 (2000) 178–181.
[27] N.V. Lisitza, Y.-Q. Song, The behavior of diffusion eigenmodes in the presence of internal magnetic field in porous media, J. Chem. Phys. 114 (2001) 9120–9124.
[28] N.V. Lisitza, Y.-Q. Song, Manipulation of the diffusion eigenmodes in porous media, Phys. Rev. B 65 (2002) 1724061–1724064.
[29] D.A. Yablonskiy, E.M. Haacke, Theory of NMR signal behavior in magnetically inhomogeneous tissues: the static dephasing regime, Magn. Reson. Med. 32 (1994) 749–763.
[30] R.M. Weisskopf, C.S. Zuo, J.L. Boxerman, B.R. Rosen, Microscopic susceptibility variation and transverse relaxation: theory and experiment, Magn. Reson. Med. 31 (1994) 601–610.
[31] D.A. Yablonskiy, Quantitation of intrinsic magnetic susceptibility-related effects in a tissue matrix, Magn. Reson. Med. 39 (1998) 417–428.
[32] P.W. Kuchel, C.J. Durrant, Permeability coefficients from NMR q-space data: models with unevenly spaced semi-permeable parallel membranes, J. Magn. Reson. 139 (1999) 258–272.
[33] V.G. Kiselev, S. Posse, Analytical model of susceptibility-induced signal dephasing: effect of diffusion in a microvascular network, Magn. Reson. Med. 41 (1999) 499–509.
[34] A.L. Sukstanskii, D.A. Yablonskiy, Theory of FID NMR signal dephasing induced by mesoscopic magnetic field inhomogeneities in biological systems, J. Magn. Reson. 151 (2001) 107–117.
[35] C.J. Durrant, M.P. Hertzberg, P.W. Kuchel, Magnetic susceptibility: further insight into macroscopic and microscopic fields and sphere of Lorentz, Concept. Magn. Reson. 18A (2003) 72–95.
[36] M.D. Herbst, J.H. Goldstein, Monitoring red blood cell aggregation with nuclear magnetic resonance, Biochem. Biophys. Acta 805 (1984) 123–126.
[37] R.J.S. Brown, Distribution of fields from randomly placed dipoles: free-precession signal decay as a result of magnetic grains, Phys. Rev. 121 (1961) 1379–1381.
[38] B. Audoly, P.N. Sen, S. Ryu, Y.-Q. Song, Correlation functions for inhomogeneous magnetic field in random media with application to a dense random pack of spheres, J. Magn. Reson. 164 (2003) 154–159.
[39] Y.-Q. Song, Using internal magnetic fields to obtain pore size distributions of porous media, Concept. Magn. Reson. 18A (2003) 97–110.
[40] E.L. Hahn, Spin echoes, Phys. Rev. 80 (1950) 580–594.
[41] Y.-Q. Song, E.E. Sigmund, N.V. Lisitza, NMR pore size measurements using internal magnetic field in porous media, in: S. Stapf, S. Han (Eds.), Nuclear Magnetic Resonance Imaging in Chemical Engineering, Wiley-VCH, London, 2005.
[42] A. Bifone, Y.-Q. Song, R. Seydoux, R.E. Taylor, B.M. Goodson, T. Pietra, T.F. Budinger, G. Navon, A. Pines, NMR laser-polarized xenon in human blood, Proc. Natl. Acad. Sci. 93 (1996) 12932–12935.
[43] M. Murayama, Orientation of sickled erythrocytes in a magnetic field, Nature 206 (1965) 420–422.
[44] T. Higashi, A. Yamagishi, T. Takeushi, N. Kawagushi, S. Sagawa, S. Onishi, M. Date, Orientation of erythrocytes in a strong magnetic field, Blood 82 (1993) 1328–1334.
[45] T. Higashi, A. Yamagishi, T. Takeushi, M. Date, Effects of static magnetic fields on erythrocyte rheology, Bioelectrochem. Bioenerg. 36 (1995) 101–108.
[46] P.T. Callaghan, A. Coy, D. MacGowan, K.J. Packer, F.O. Zelaya, Diffraction-like effects in NMR diffusion studies of fluids in porous solids, Nature 351 (1991) 467–469.
[47] A.M. Torres, A.T. Taurins, D.G. Regan, B.E. Chapman, P.W. Kuchel, Assignment of coherence features in NMR q-space plots to particular diffusion modes in erythrocyte suspensions, J. Magn. Reson. 138 (1999) 135–143.
[48] D.G. Regan, P.W. Kuchel, NMR studies of diffusion-coherence phenomena in red cell suspensions: current status, Israel J. Chem. 43 (2003) 45–54.
[49] L.J. Zielinski, Y.-Q. Song, S. Ryu, P.N. Sen, Characterization of coupled pore systems from the diffusion eigenspectrum, J. Chem. Phys. 117 (2002) 5361–5365.
[50] L. Venkataramanan, Y.-Q. Song, M.D. Hurlimann, Solving Fredholm integrals of the first kind with tensor product structure in 2 and 2.5 dimensions, IEEE Tran. Signal Proc. 50 (2002) 1017–1026.
[51] D.L. Rabenstein, ^{1}H NMR methods for the non-invasive study of metabolism and other processes involving small molecules in intact erythrocytes, J. Biochem. Biophys. Method. 9 (1984) 277–306.
[52] E. Humpfer, M. Spraul, A.W. Nicholls, J.K. Nicholson, J.C. Lindon, Direct observation of resolved intra-cellular and extra-cellular water signals in intact human red blood cells using ^{1}H MAS NMR spectroscopy, Magn. Reson. Med. 38 (1997) 334–336.
[53] K.R. Brownstein, C.E. Tarr, Importance of classical diffusion in NMR studies of water in biological cells, Phys. Rev. A 19 (1979) 2446–2453.
[54] G.T. Rick, R.I. Sha'afi, T.C. Barton, A.K. Solomon, Permeability studies on red cell membrane of dog, cat, and beef, J. Gen. Physiol. 50 (1967) 2391–2405.
[55] G. Benga, H. Matei, L. Frentescu, B.E. Chapman, P.W. Kuchel, Comparative nuclear magnetic resonance studies of diffusional water permeability of red blood cells from different species. XI. Horses introduced to Australia and European horses (Equus caballus), Comp. Haemtol. Int. 10 (2000) 138–143.

[56] G. Benga, S.M. Grieve, B.E. Chapman, C.H. Gallagher, P.W. Kuchel, Comparative MMR studies of diffusional water permeability of red blood cells from different species. X. Camel (Camelus dromedarius) and alpaca (Lama pacos), Comp. Haemtol. Int. 9 (1999) 43–48.

[57] G. Benga, T. Borza, H. Matei, P. Hodor, L. Frentescu, I. Ghiran, C. Lupse, Comparative nuclear magnetic resonance studies of diffusional water permeability of red blood cells from different species. 8. Adult and fetal guinea-pig (Cavia-Procellus), Comp. Haemtol. Int. 5 (1995) 106–111.

[58] G. Benga, H. Matei, T. Borza, D. Poruitiu, C. Lupse, Comparative MMR studies of diffusional water permeability of red blood cells from different species. 5. Rabbit (Oryctolagus-Cuniculus), Compar. Biochem. Physiol. B: Biochem. Mol. Biol. 106 (1993) 281–285.

[59] G. Benga, T. Borza, O. Popescu, D. Poruitiu, H. Matei, Comparative MMR studies of diffusional water permeability of red blood cells from sheep and cow, Compar. Biochem. Physiol. B: Biochem. Mol. Biol. 104 (1993) 589–594.

[60] G. Benga, H. Matei, T. Borza, D. Poruitiu, C. Lupse, Comparative MMR studies of diffusional water permeability of red blood cells from mice and rats, Compar. Biochem. Physiol. A: Physiology 104 (1993) 491–495.

[61] H.C. Torrey, Bloch equations with diffusion terms, Phys. Rev. 104 (1956) 563–565.

[62] K.R. Brownstein, C.E. Tarr, Spin–lattice relaxation in a system governed by diffusion, J. Magn. Reson. 26 (1977) 17–24.